ACS SENSORS

Article

Cite This: ACS Sens. 2019, 4, 3034−3041

pubs.acs.org/acssensors

Microcantilever Array Biosensor for Simultaneous Detection of Carcinoembryonic Antigens and α-Fetoprotein Based on Real-Time Monitoring of the Profile of Cantilever

Chen Li,[†,‡] Xingxing Ma,[†,‡] Yanxue Guan,[†,‡] Jilin Tang,*[,†,‡] and Bailin Zhang*[,†,‡]

[†]State Key Laboratory of Electroanalytical Chemistry, Changchun Institute of Applied Chemistry, Chinese Academy of Sciences, Changchun 130022, P. R. China

[‡]University of Science and Technology of China, Hefei 230026, P. R. China

Supporting Information

ABSTRACT: A microcantilever array biosensor based on a sandwich structure has been developed for simultaneously measuring two biomarkers carcinoembryonic antigen (CEA) and α-fetoprotein (AFP) via an optical readout technique—real-time monitoring of the profile of cantilever. First, the aptamers of CEA and AFP were self-assembled on their respective cantilevers. After the adsorption of the mixture of CEA and AFP, further specific interaction was performed via the addition of the antibodies specific to each target. The compressive stress on the cantilever was generated by the aptamer−antigen−antibody sandwich structure formed on the gold surface, resulting in cantilever bending. The profile of cantilever could be monitored in real time. The relationship between the deflection value at the 90% position of the cantilever and the target concentration served as a calibration curve, and the detection sensitivity was 1.3 ng/mL for CEA and 0.6 ng/mL for AFP, respectively. This work demonstrated the ability of simultaneously measuring two biomarkers via a microcantilever array biosensor, giving great potential for further application in detecting several targets simultaneously for early clinical diagnosis.

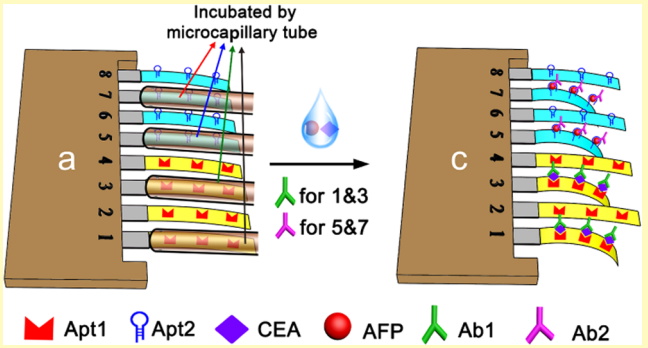

KEYWORDS: *microcantilever array biosensor, sandwich structure, simultaneous measurement, biomarkers, profile*

The rapid and sensitive determination of tumor biomarkers, such as serum tumor markers and potential prognostic factors, is a critical clinical issue in the diagnosis and treatment of tumor-associated diseases.[1,2] However, single biomarker detection has failed to meet clinical needs since it can easily lead to false positive results in tumor diagnosis compared with multiplex biomarker detection.[3,4] On the other hand, a depressed or elevated concentration of many protein biomarkers is usually associated with more than one kind of cancer or disease forms.[5] Thus, it is necessary to simultaneously detect more biomarkers in methodologies developed for successful prediction of cancer and other diseases.

Until now, the multiplex methods for clinical biomarker measurements have been studied extensively. The enzyme-linked immunosorbent assay, which is the most common and widely used technology, has been considered to be the gold standard for many proteins.[6−9] Other methods, such as an immunosensor based on electrochemiluminescence,[10,11] surface-enhanced Raman spectroscopy,[12] and electrochemistry,[13,14] have also been reported to detect various biomarkers. However, these approaches have disadvantages of small sample size, relatively expensive reagent cost, and the need to label signal molecules, which limits their application in multiplexing.

Microcantilever array sensing technology, originated from atomic force microscopy[15] and developed in the 1990s, provides a new analytical platform with high throughput, selectivity and sensitivity, label-free detection, and low cost. Its sensing unit usually has a micron-sized rectangular cantilever beam coated with a sensitive layer on the one side. The analytes can interact with sensitive layer which can cause a bending signal[16] or frequency changes[17] of the cantilever. This micrometer size demands short response times and low sample volumes.[18] As well as combined with modern semiconductor processing technology, the microcantilever array can be parallel integration and mass-produced at a lower cost. Thus, microcantilever array-based biosensor exhibits extremely high sensitivity in mass and stress measurements[19] and offers the possibility of simultaneous detection of multiple samples.

Several studies have been focused on measuring more than one analytes by this cantilever array. Jeon et al.[20] used a silicon microcantilever array immunoassay based on magnetic photocatalytic hybrid nanoparticles with a highly crystalline TiO_2

Received: August 19, 2019
Accepted: October 23, 2019
Published: October 23, 2019

DOI: 10.1021/acssensors.9b01604
ACS Sens. 2019, 4, 3034−3041

Scheme 1. (A) Schematic Illustration of the Detection Principle for the Simultaneous Detection of Two Biomarkers CEA and AFP by the Microcantilever Array Biosensor, (B) Diagram of Microcantilever Array Grouping Modification, and (C) Schematic Depiction of the Readout Technique for Real-Time Profiling of Cantilever Arrays; Not Drawn to Scale

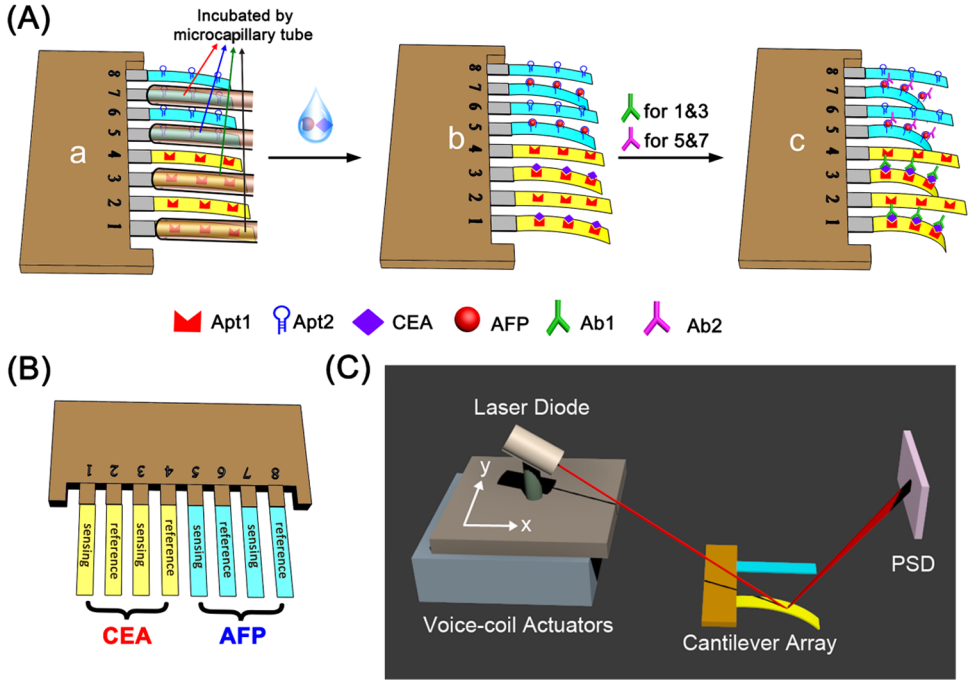

shell for sensitive measurement of several protein biomarkers. Yang and his co-workers[21] used a pillar array-based microcavity detecting multiple liver cancer biomarkers via antibody-antigen interaction. In these methods, dynamic mode in the air is commonly used. However, air may destroy the physiological environment of the protein. In the liquid, the performance of dynamic mode was severely reduced due to damping.[22] Therefore, based on microcantilever array sensor, simultaneous detection of multiple biomolecules in a liquid environment is urgent for us to study.

Carcinoembryonic antigen (CEA), a member of family of cell surface glycoproteins, is largely overexpressed in essentially all human colon carcinomas and in a high proportion of cancers at many other sites.[23,24] α-Fetoprotein (AFP) is an oncofetal glycoprotein, and the average level of AFP in the healthy human serum was less than 25 ng/mL, while an extremely high level can be found in the serum of patients experiencing primary liver cancer.[25,26] Due to their relevance to tumor malignant metastasis, they are widely used as tumor markers, which also aroused considerable interest in detecting them. Herein, we constructed a sandwich-based microcantilever array biosensor for simultaneous detection of two biomarkers CEA and AFP in liquid by monitoring the profile of cantilever at the static mode, as shown in Scheme 1A. First, we divided the microcantilever array into two groups according to Scheme 1B; one group is the cantilevers 1−4 as for detecting CEA, while the other one is the cantilevers 5−7 as for detecting AFP. Among them, 1, 3 and 5, 7 are the sensing cantilevers and 2, 4 and 6, 8 are the reference ones. Then, CEA aptamers (Apt1) and AFP aptamers (Apt2), which can bind to their respective ligands CEA and AFP, were self-assembly immobilized on their cantilevers, respectively. When the mixture of CEA and AFP is present, the interaction between targets and their respective aptamers gives rise to cantilever bending. We scale up the signal by introducing each antibody as part of a multiplexed sandwich assay on the cantilever chip surface after exposure to the target proteins. The cantilever deflection profiles amplified by sandwich structure were detected by a scanning laser analyzer (SCALA). It is particularly promising for this microcantilever array assay to detect different targets simultaneously in biochemical analysis and clinical research.

EXPERIMENTAL SECTION

Materials and Reagents. The rectangular gold-coated microcantilever array with eight identified cantilevers was obtained from Shanghai NTI Co., Ltd. (Shanghai, China). Figure S1 shows the structure of the cantilever array chip by scanning electron microscopy (SEM). Single cantilever length is 500 μm, width is 90 μm, and thickness is 1 μm, as shown in enlargement of Figure S1. CEA, AFP, detection antibodies against each Ab1 and Ab2, prostatic specific antigen (PSA), human serum albumin (HSA), and bovine serum albumin (BSA) were purchased from Shanghai Linc-Bio Science Co., Ltd. Both the 5′-mercapto-modified DNA aptamer 1(Apt1) specific to CEA, whose sequence is 5′-(SH)-$(CH_2)_6$-ATA CCA GCT TAT TCA ATT-3′, and the 5′-mercapto-modified DNA aptamer 2(Apt2) specific to AFP, whose sequence is 5′-(SH)-$(CH_2)_6$-GGC AGG AAG ACA AAC AAG CTT GGC GGC GGG AAG GTG TTT AAA TTC CCG GGT CTG CGT GGT CTG TGG TGC TGT-3′, were synthesized by Sangon Biotechnology (Shanghai, China). Tris(2-carboxyethyl) phosphine hydrochloride (TCEP, Alfa Aesar) and 6-mercapto-1-hexanol (MCH, Sigma-Aldrich, St. Louis, MO) were used as purchased without any further purification. All chemicals used in this study were of analytical reagent grade. All of the experimental water was deionized water (18.2 MΩ cm^{-1}) from a Milli-Q water purification system (Millipore).

Apparatus and Instruments. All functionalization of the microcantilever was performed by Functionalization Unit Operating Instructions from the Cantisens Research Cantilever Array System. The deflection measurements were obtained with a scanning laser analyzer (SCALA, Mecwins, Spain). The topography of the micorcantilever array was determined on a Philips XL30 ESEM FEG and a scanning electron microscope (SEM, Jeol Inc.). X-ray

DOI: 10.1021/acssensors.9b01604
ACS Sens. 2019, 4, 3034−3041

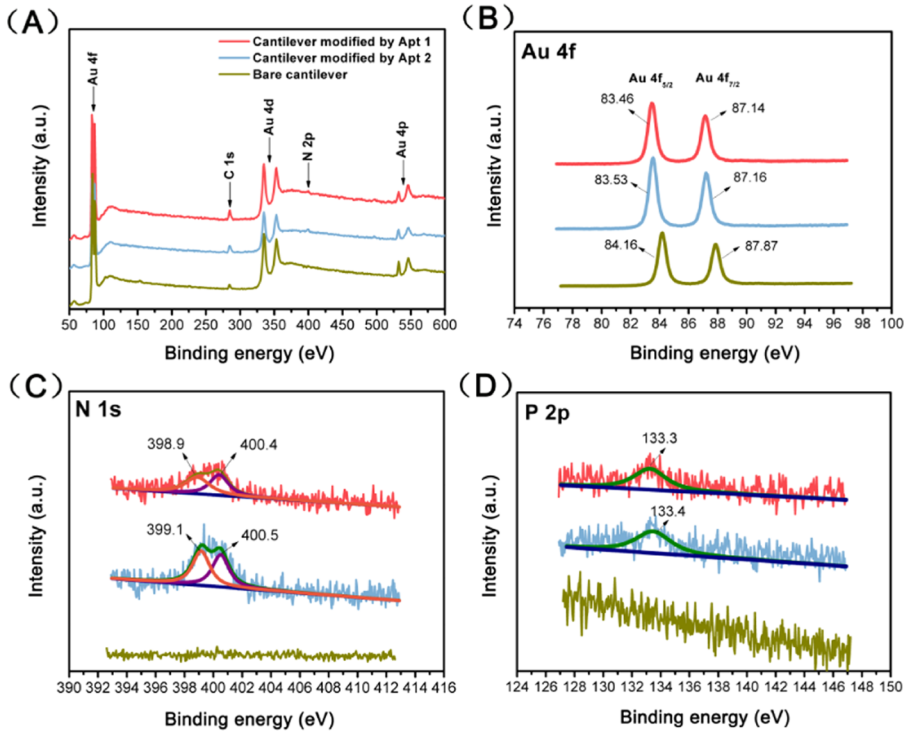

Figure 1. (A) Representative XPS survey spectra obtained for each functionalization step of the cantilevers. High-resolution XPS spectra of (B) Au 4f, (C) N 1s, and (D) P 2p core level of functionalizing microcantilevers obtained for each functionalization step; modified by Apt1 (red), modified by Apt2 (blue), and bare cantilever (green).

photoelectron spectroscopy (XPS) experiments were conducted using an ESCALABMK II X-ray photoelectron spectrometer using Mg as the excitation source.

Immobilization of Aptamers on the Microcantilever. The Apt1 and Apt2 were predissolved in 10 mM Tris−HCl containing 1 mM TCEP (pH 7.4) buffer, respectively. Before functionalization, the microcantilever array was cleaned by piranha solution (Caution! the piranha solution is strongly corrosive and must be handled carefully.) for 60 s and exposed to an ultraviolet ozone environment for 30 min to remove organic and inorganic contaminants. Then, the microcantilever was washed 3 times by Milli-Q water and ethanol, respectively, and dried by nitrogen gas for next functionalization. First, the array was divided into two groups: in cantilevers 1−4 were inserted four microcapillaries filled with 1 μM Apt1 solution in parallel separately as CEA cantilevers and the other cantilevers 5−8 were with Apt2 solution as AFP cantilevers. Then, the array was rinsed 3 times by PBS to eliminate the excess aptamers. Afterward, the whole microcantilever array was immersed in 1 mM MCH for 1 h to occupy other remaining sites. Finally, the array was rinsed 3 times by PBS and dried by nitrogen.

Experiment Protocol for Detecting Biomarkers. The fabrication procedure of the microcantilever array was operated independently by capillary method modifications. Twenty-five microliter of solution mixed with different concentrations of CEA and AFP (0.01 M PBS, pH 7.4) was reacted with aptamers on the cantilevers (1, 3, 5, and 7) and incubated for 1 h at room temperature by microcapillary tubes, and then, the array was washed extensively to remove unbound molecules. Next, 1 μg/mL Ab1 solution (0.01 M PBS, 0.15 M NaCl, pH 7.4) was functionalized onto the surface of cantilevers 1 and 3 and 1 μg/mL Ab2 solution (0.01 M PBS, 0.15 M NaCl, pH 7.4) on the surface of cantilevers 5 and 7 and then incubated for another 1 h. The other cantilevers (2, 4, 6, and 8) were reference ones. Finally, the array was rinsed by PBS and dried by nitrogen and ready for measurement. The steps of the deflection detection in the real sample are consistent with that in PBS solution, except for using 10% human serum as a hybridization and reaction buffer. It should be noted that the differential deflection profiles are obtained by subtracting the deflection of the reference cantilever from the sensing cantilever deflection and will not be described later.

RESULTS AND DISCUSSION

Detection Principle of This Assay. In this work, we used an optical readout technique for the profile measurement of microcantilever array by real-time measuring of the displacement and motion of plurality of selected locations of a mechanical structure or of a region of interest of that structure.[27] This system overcomes the challenge of assumption of simplistic models to reduce stress of the cantilever from the displacement measurement in the optical beam deflection technique, which is based on a single laser point measurement at the cantilever free end.[28,29] The special element of this readout technique is that a single laser beam by mounting on the two perpendicular linear voice-coil actuators can be automatically scanned in two dimensions, as shown in Scheme 1C. The laser emitted from the 3 mW laser diode can perform two-dimensional nonhysteretic displacement over a range of several millimeters, whose speed can be up to 50 mm/s and accuracy is 100 nm. To obtain the cantilever profile, two scan trajectories are carried out in the microcantilever array. One is perpendicular to the longitudinal cantilever axis to confirm the position of the cantilever. The other one is along the longitudinal cantilever axis to obtain the cantilever profiles. When the laser beam shines onto the cantilever array directly, its trajectory can be gathered by a two-dimensional linear position-sensitive detector (PSD). The profile of each cantilever can be described by the following formula: $z(x) = \frac{1}{2D}\int_x^0 s(x')\,dx' - \frac{1x^2}{4D}\cos\beta$, where $z(x)$ is the cantilever profile along its longitudinal axis, D is the distance between the cantilever and PSD, $s(x)$ is the displacement

DOI: 10.1021/acssensors.9b01604
ACS Sens. 2019, 4, 3034−3041

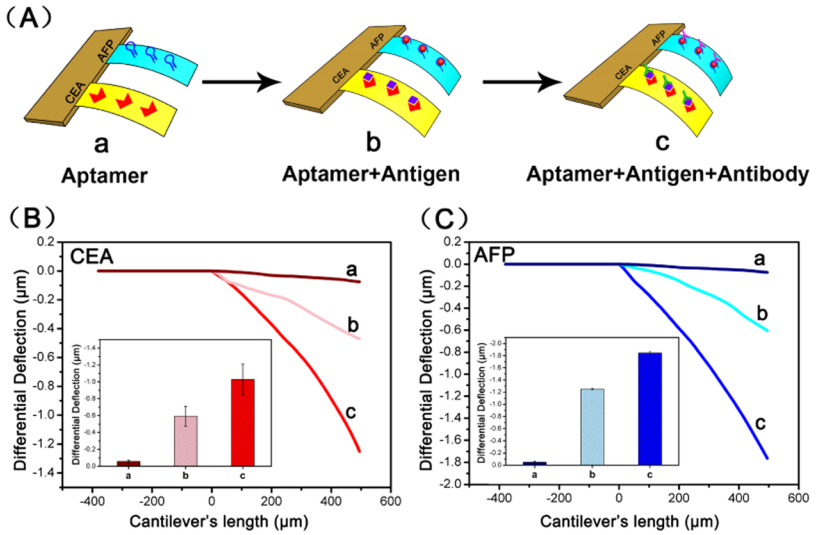

Figure 2. Differential deflection for the cantilever modified by different steps. (A) Schematic diagram of microcantilever biosensor at each modification step. Differential deflection profiles of (B) CEA microcantilever and (C) AFP microcantliever, where curves *a*, *b*, and *c* represented the differential deflection of cantielvers modified by aptamers, mixture of CEA and AFP, and antibodies to each target, respectively. (The insets are the corresponding histograms of the deflection values collected at the 90% position of the cantilever.)

recorded by the PSD, and β is the angle between the incident laser beam and the cantilever normal at its rest position.

At the beginning, we defined the deflection caused by compressive surface stress, i.e., as negative, where the microcantilever bends downward to the silicon side. As both of DNA aptamers and antibodies are capable of binding to CEA and AFP simultaneously via different epitope sites, the sandwich structure based on aptamer−target−antibody was successfully established on the cantilever surface. In addition, due to the tight binding between aptamers and target on the cantilever surface, the bulky aptamer−target complex leads to the expansion of the molecular layer on the microcantilever and the increase of molecular repulsion.[30] Furthermore, the addition of antibodies enhances this effect tremendously. Eventually, the microcantilever bends toward the silicon surface with a large negative deflection and the profiles of each cantilever can be detected individually and sequentially.

Characterization of the Microcantilever Array Biosensor. XPS spectra were employed to characterize the aptamer monolayers immobilized on the gold surface of the sensor. By irradiating X-ray on a bare cantilever and cantilever modified by Apt1 or Apt2, the high-resolution XPS spectra were obtained, as shown in Figure 1. Figure 1A shows the corresponding XPS survey spectra. The analysis of the shape of the spectra, which is generated by exciting electrons in specific bound states and measuring the kinetic energy that electrons escape from the near-surface structure, clearly revealed the formation of a self-assembled monolayer (SAM) on the gold surface.[31] The Au 4f electrons in Figure 1B exhibited two characteristic peaks, which correspond to the Au $4f_{5/2}$ and Au $4f_{7/2}$ orbitals, respectively. We can see there are −0.6 to −0.7 eV shifts of binding energy (BE) on the cantilever modified by Apt1 and Apt2 compared with the spectrum of the bare cantilever. This is because Au atoms on the bare cantilever surface are partially oxidized, causing a counteracting shift to a higher BE corresponding to Au(0) (83.9 ± 0.1 eV).[32] While for the cantilever modified by Apt1 or Apt2, the negative shift arises from a combination of the surface atoms due to the formation of the Au−S bond.[33] Figure 1C shows the high-resolution XPS spectra of N 1s. On cantilevers modified by Apt1 and Apt2, there exhibited two characteristic peaks at about 399.0 and 400.5 eV, which are assigned to conjugated N (sp^2) and the mixture of amine group $-NH_2$, nonconjugated N (sp^3), and N−(C═)−N, respectively.[33−35] This is attributed to the location of nitrogen atoms in an aromatic ring structure in DNA bases.[36,37] Similar to the nitrogen atom, the binding energy of P 2p for the cantilever modified by Apt1 and Apt2 in Figure 1D was about 133.4 eV, which is the characteristic peak of phosphate in the DNA backbone.[35] However, for the bare cantilever, no characteristic peak of nitrogen or phosphorus was observed. In short, all XPS experiments confirmed that the SAM layer has been successfully immobilized on the gold surface.

To confirm that the constructed sandwich structure can improve the detection sensitivity, each stepwise construction process of the microcantilever array biosensor was characterizated by SCALA, as shown in Figure 2. Figure 2A illustrates the schematic diagram of each modification step for the cantilever array chip, while Figure 2B,C represents the deflections of the profiles of the cantilever of CEA and AFP at different modified states, respectively. When the cantilever was only modified by aptamers, the profiles of both CEA and AFP cantilevers (curve *a* in Figure 2B,C) have only a slight negative deflection by deducting the deflection value of reference cantilever and the deflection values at the 90% position of the cantilever are −0.059 and −0.048 μm, respectively. After induction with the target mixture of CEA and AFP, the profiles of the CEA and AFP cantilever have a significant negative deflection (curve *b* in Figure 2B,C) and the deflection values at the 90% position of the cantilever are −0.59 and −1.25 μm, respectively. Compared with the cantilever modified only by the aptamer, the deflection values are increased by 10 and 26 times, respectively. The reason is that the interaction of targets and their aptamers results in an increase in the compressive stress on the cantilever surface, generating in a large bend in the cantilever. Finally, followed by the CEA and AFP sensing cantilevers continuously interacting with Ab1 and Ab2, respectively, the profile of the cantilever is

DOI: 10.1021/acssensors.9b01604
ACS Sens. 2019, 4, 3034−3041

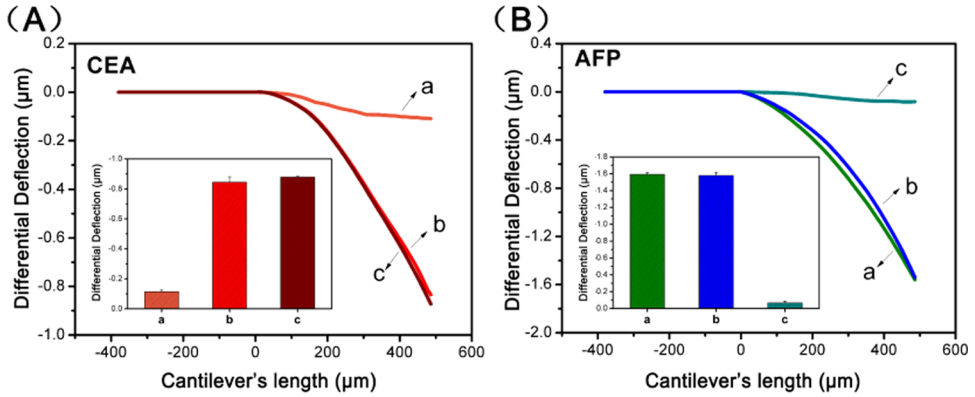

Figure 3. Evaluation of cross activity of the microcantilever array biosensor for simultaneous detection of two biomarkers. Differential deflection profile of (A) CEA microcantilever and (B) AFP microcantliever, where curves *a*, *b*, and *c* were only 500 ng/mL AFP, 500 ng/mL mixture of CEA and AFP, and only 500 ng/mL CEA, respectively. (The insets are the corresponding histograms of the deflection values collected at the 90% position of the cantilever.)

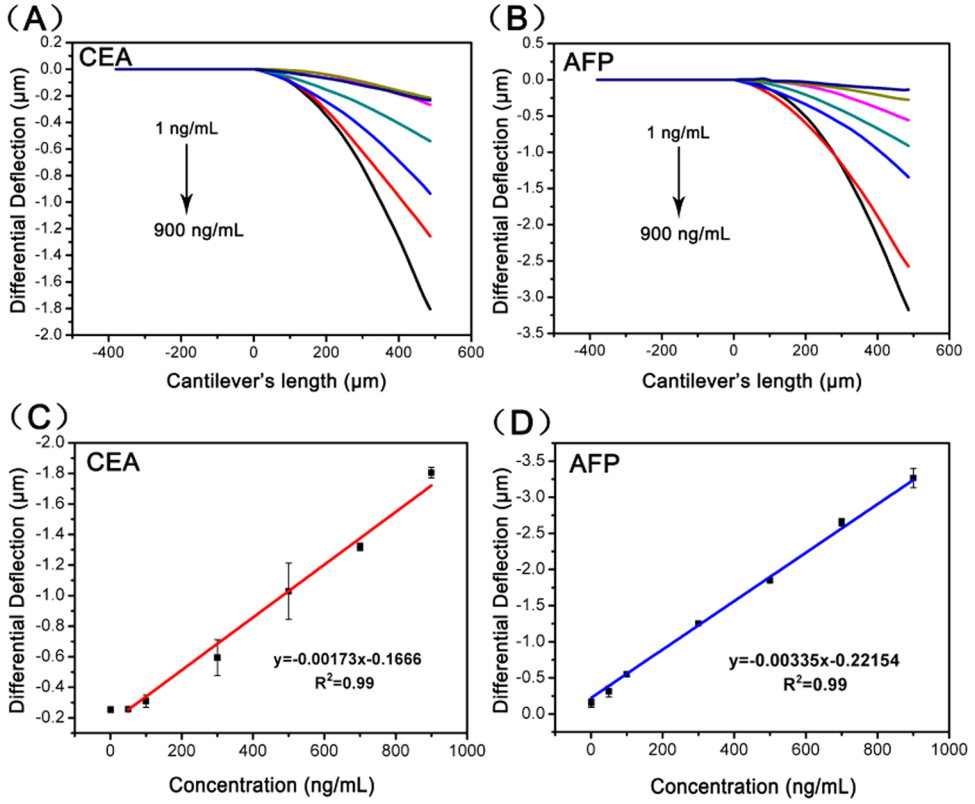

Figure 4. Differential deflections of whole cantilever for detecting CEA (A) and AFP (B) at different concentrations. (B) Calibration plot for CEA (C) and AFP (D) detection by selecting the deflection at the cantilever tip 90% position. The error bars represent the standard deviation of data (n = 3).

further negatively deflected (curve *c* in Figure 2B,C) and the deflection values at the 90% position of the cantilever are −1.03 and −1.85 μm, respectively. The defelction values are increased by 17 times and 38 times, respectively. This is because the Abs is successfully fixed on the cantilever, forming an aptamer−target−Ab sandwich structure and further enhancing the compressive stress on the surface of the cantilever. These experiments have fully confirmed that the microcantilever array sensor with sandwich construction can indeed enhance the simultaneous detection of CEA and AFP signals.

Feasibility of the Microcantilever Array Biosensor. The feasibility of the proposed assay was estimated by investigating the ability of resistance to interference. We performed cross-interference tests by adding only different detection targets without changing other experimental conditions. The targets were 500 ng/mL AFP, 500 ng/mL AFP and CEA mixture, and 500 ng/mL AFP, respectively. The cantilever deflections caused by these targets corresponded to *a*, *b*, and *c* in Figure 3. For the CEA cantilever, it can be clearly seen that, when the target is only 500 ng/mL AFP (curve *a* in Figure 3A), only a slight deflection is produced and the deflection value at 90% position of the cantilever is −0.11 μm.

DOI: 10.1021/acssensors.9b01604
ACS Sens. 2019, 4, 3034−3041

While the target is the mixture of CEA and AFP (curve *b* in Figure 3A), a great deflection was generated and the deflection profile is almost coincident with the detection of only 500 ng/mL CEA (curve *b* in Figure 3A). The deflection value achieved at the 90% position of the cantilever is −0.85 μm, which is comparable to that of only a single component of CEA (the deflection value is −0.87 μm). Similarly, for the AFP cantilever, as shown in Figure 3B, when the target was only CEA (curve *c* in Figure 3B), the deflection of the cantilever is very small and the deflection value at the 90% position is only −0.066 μm. When the target is mixture of CEA and AFP (curve *b* in Figure 3B), the deflection profile of the cantilever is bending drastically, which is almost similar to that when only 500 ng/mL AFP is detected (curve *a* in Figure 3B), and the deflection value of the cantilever 90% position can reach −1.58 μm (the deflection value is only −1.59 μm when only AFP is detected). In other words, the differential deflection response reveals that the sensor we built has only a small difference between detecting a single target or a mixture of two targets, which are negligible. Therefore, our microcantilever array sensor can detect two targets at the same time without interfering with each other.

Analytical Performance for Quantitative Simultaneous Detection of CEA and AFP. To examine the sensitivity of the sandwich-based microcantilever array biosensor for quantitative determination of CEA and AFP simultaneously, the deflections induced by a series of different concentrations of CEA and AFP were investigated, as shown in Figure 5 under the optimized condition. Figure 4A,B shows the differential deflection profiles of the whole cantilever for detecting CEA and AFP at different concentrations, respectively. As shown in the figure, with the increase in concentration, both deflection values increased. The relationship between the deflection value at the 90% position of the cantilever and the concentration was proportional and is plotted in Figure 4C,D. The linear ranges for measuring CEA and AFP were from 50 to 900 and 1 to 900 ng/mL with detection limits of 1.3 and 0.6 ng/mL at $S/N = 3$, respectively. The comparison with other reported methods for the detection of CEA and AFP is displayed in Table S1, and the detection limit and linear range are comparable. Therefore, the proposed sandwich-based microcantilever array aptasensor for the quantitative determination of CEA and AFP simultaneously was fairly worthy.

To evaluate the selectivity of the cantilever array biosensor for simultaneous detection of CEA and AFP, control experiments were investigated by determining other various biomarker proteins, including BSA, HSA, PSA, and mucin 1. Figure 5 shows a comparison of the deflection values of BSA, HSA, PSA, and mucin 1 on the CEA and AFP cantilever sensor, respectively. It is clearly displayed that other proteins only led to almost negligible deflection at the same concentration (500 ng/mL) compared with CEA and AFP. This may because their aptamer−antibody system has a higher affinity and selectivity for the analytes than other proteins. Thus, the obtained results confirmed that the cantilever array biosensor had high selectivity for codetermination of the two targets CEA and AFP.

Reproducibility and Stability of Cantilever Array Biosensor. To evaluate the reproducibility of the fabricated microcantilever array biosensor, three different microcantilever array biosensors were constructed using the same fabrication protocol for detecting a mixture containing 500 ng/mL CEA and AFP and the deflections were assessed. As demonstrated in

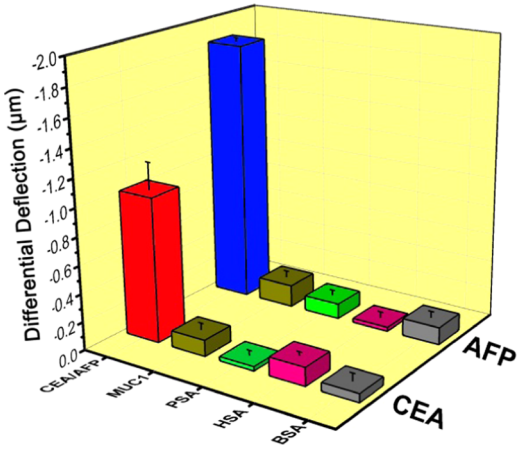

Figure 5. Selectivity of the cantilever array biosensor for simultaneous detection of CEA and AFP. The concentrations of biomarkers are 500 ng/mL. The error bars represent the standard deviation of data (n = 3).

Figure 6A, differential deflection measurements were recorded for CEA (red solid circles) and AFP (blue solid squares) and yielded the RSD values of 1.18 and 4.63%, respectively, confirming a rather good reproducibility of the proposed cantilever array biosensor. To investigate the signal stability of the proposed microcantilever array biosensor, we measured the deflection signal six times in succession. As shown in Figure S3, the standard deviation of the six measurements was less than 3%. Furthermore, the time stability of the proposed sensor was also examined by monitoring the deflection response after storing in PBS, pH 7.4, at 4 °C for 2 days. As shown in Figure 6B, with the storage time increasing, the differential deflection values of CEA and AFP are slightly attenuated, but the signal attenuation is less than 10%, which suggests that the stability of the proposed biosensor is acceptable.

Serum Sample Analysis of the Microcantilever Array Biosensor. Finally, we investigated the potential application of this microcantilever array sensor in practical samples. We used a standard addition method by adding 50, 100, and 500 ng/mL mixture of CEA and AFP in PBS containing 10% serum for the determination of recovery experiments. The average recovery of the sensor was calculated, and the results are shown in Table S2. The result manifested that the recoveries were in a range of 113−118% for CEA and 101−113% for AFP, respectively, which indicates that this method has high reliability and accuracy for the simultaneous detection of two analytes in serum samples and is promising for clinical testing.

CONCLUSIONS

In summary, a microcantilever array biosensor for simultaneous detection of two biomarkers CEA and AFP by the aptamer−antibody sandwich assay has been constructed. There are three novel points in this method. First, two biomarkers are simultaneously determined via the characteristic of multiple arrays of microcantilevers. Second, the sensitivity has been enhanced by the aptamer−antigen−antibody sandwich immunoassay. Finally, this approach employs a readout technology—real-time monitoring of the profile of the cantilever. This readout technique provides absolute values of the cantilever profile rather than relative variations of the local slope in less than 1 s. Moreover, compared with the conventional optical beam deflection

DOI: 10.1021/acssensors.9b01604
ACS Sens. 2019, 4, 3034−3041

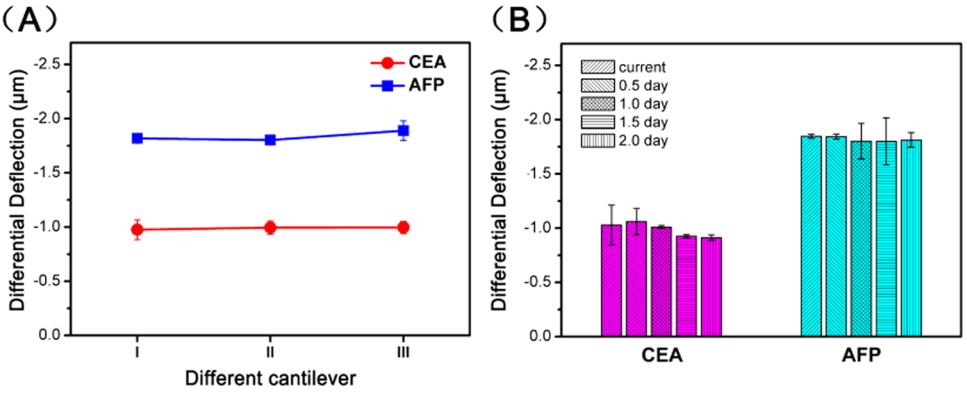

Figure 6. (A) Reproducibility evaluation of the cantilever array biosensor under three different cantilevers constructed by the same procedure, in which the cantilever was detected 3 times. (B) Stability evaluation of the microcantilever array biosensor stored in PBS at 4°C for 2 days.

techniques, the resulting cantilever profile provides more comprehensive reaction information about the cantilever surface. In future, we fully believe that this microcantilever array sensing system could be applied in simultaneous detection of a variety of targets in biochemical research and clinical diagnosis.

■ ASSOCIATED CONTENT

Supporting Information

The Supporting Information is available free of charge on the ACS Publications website at DOI: 10.1021/acssensors.9b01604.

SEM image of the microcantilever array; optimal experiments for aptamer concentration; signal stability of the microcantilever biosensor; consecutive measurement for 6 times; and analytical results of CEA and AFP in serum samples (PDF)

■ AUTHOR INFORMATION

Corresponding Authors

*E-mail: jltang@ciac.ac.cn. Tel/Fax: +86-0431-85262734. (J.T.).

*E-mail: blzhang@ciac.ac.cn. Tel/Fax: +86-0431-85262430. (B.Z.).

ORCID

Jilin Tang: 0000-0002-8515-5495

Bailin Zhang: 0000-0002-8114-2590

Notes

The authors declare no competing financial interest.

■ ACKNOWLEDGMENTS

This study was supported by the National Natural Science Foundation of China (Nos. 21375122 and 21775144).

■ REFERENCES

(1) Wu, J.; Fu, Z.; Yan, F.; Ju, H. Biomedical and clinical applications of immunoassays and immunosensors for tumor markers. *TrAC, Trends Anal. Chem.* **2007**, *26*, 679−688.

(2) Faraggi, D.; Kramar, A. Methodological issues associated with tumor marker development: Biostatistical aspects. *Urol. Oncol.: Semin. Orig. Invest.* **2000**, *5*, 211−213.

(3) Kulasingam, V.; Diamandis, E. P. Strategies for discovering novel cancer biomarkers through utilization of emerging technologies. *Nat. Clin. Pract. Oncol.* **2008**, *5*, 588−599.

(4) Ludwig, J. A.; Weinstein, J. N. Biomarkers in cancer staging, prognosis and treatment selection. *Nat. Rev. Cancer* **2005**, *5*, 845−856.

(5) Munge, B. S.; Stracensky, T.; Gamez, K.; DiBiase, D.; Rusling, J. F. Multiplex immunosensor arrays for electrochemical detection of cancer biomarker proteins. *Electroanalysis* **2016**, *28*, 2644−2658.

(6) Rusling, J. F. Multiplexed electrochemical protein detection and translation to personalized cancer diagnostics. *Anal. Chem.* **2013**, *85*, 5304−5310.

(7) Wang, J. Electrochemical biosensors: Towards point-of-care cancer diagnostics. *Biosens. Bioelectron.* **2006**, *21*, 1887−1892.

(8) Li, J. N.; Zhang, Z.; Rosenzweig, J.; Wang, Y. Y.; Chan, D. W. Proteomics and bioinformatics approaches for identification of serum biomarkers to detect breast cancer. *Clin. Chem.* **2002**, *48*, 1296−1304.

(9) Heineman, W. R.; Halsall, H. B. Strategies for electrochemical immunoassay. *Anal. Chem.* **1985**, *57*, 1321A−1331A.

(10) Tang, C. K.; Vaze, A.; Shen, M.; Rusling, J. F. High-throughput electrochemical microfluidic immunoarray for multiplexed detection of cancer biomarker proteins. *ACS Sens.* **2016**, *1*, 1036−1043.

(11) Ma, C.; Liu, H.; Zhang, L.; Li, H.; Yan, M.; Song, X.; Yu, J. Multiplexed aptasensor for simultaneous detection of carcinoembryonic antigen and mucin-1 based on metal ion electrochemical labels and $Ru(NH_3)_6^{3+}$ electronic wires. *Biosens. Bioelectron.* **2018**, *99*, 8−13.

(12) Zhou, W.; Tian, Y. F.; Yin, B. C.; Ye, B. C. Simultaneous surface-enhanced raman spectroscopy detection of multiplexed microRNA biomarkers. *Anal. Chem.* **2017**, *89*, 6120−6128.

(13) Wu, J.; Zhang, Z.; Fu, Z. F.; Ju, H. X. A disposable two-throughput electrochemical immunosensor chip for simultaneous multianalyte detennination of tumor markers. *Biosens. Bioelectron.* **2007**, *23*, 114−120.

(14) Füzéry, A. K.; Levin, J.; Chan, M. M.; Chan, D. W. Translation of proteomic biomarkers into FDA approved cancer diagnostics: issues and challenges. *Clin. Proteomics* **2013**, *10*, No. 13.

(15) Binnig, G.; Quate, C. F.; Gerber, C. Atomic force microscope. *Phys. Rev. Lett.* **1986**, *56*, 930−933.

(16) Mathew, R.; Ravi Sankar, A. A review on surface stress-based miniaturized piezoresistive SU-8 polymeric cantilever sensors. *Nano-Micro Lett.* **2018**, *10*, No. 35.

(17) Bietsch, A.; Zhang, J. Y.; Hegner, M.; Lang, H. P.; Gerber, C. Rapid functionalization of cantilever array sensors by inkjet printing. *Nanotechnology* **2004**, *15*, 873−880.

(18) Berger, R.; Gerber, C.; Lang, H. P.; Gimzewski, J. K. Micromechanics: A toolbox for femtoscale science: "Towards a laboratory on a tip". *Microelectron. Eng.* **1997**, *35*, 373−379.

(19) Yi, J. W.; ShihShih, W. Y.; Shih, W. H. Wei-Heng Shih Effect of length, width, and mode on the mass detection sensitivity of piezoelectric unimorph cantilevers. *J. Appl. Phys.* **2002**, *91*, 1680−1686.

DOI: 10.1021/acssensors.9b01604
ACS Sens. 2019, 4, 3034−3041

(20) Joo, J.; Kwon, D.; Yim, C.; Jeon, S. Highly sensitive diagnostic assay for the detection of protein biomarkers using microresonators and multifunctional nanoparticles. *ACS Nano* **2012**, *6*, 4375−4381.
(21) Wang, J.; Zhu, Y.; Wang, X.; Wang, S.; Yang, J.; Yang, F. A high-throughput cantilever array sensor for multiple liver cancer biomarkers detection. *IEEE Sens. J.* **2016**, *16*, 4675−4682.
(22) Sader, J. E. Frequency response of cantilever beams immersed in viscous fluids with applications to the atomic force microscope. *J. Appl. Phys.* **1998**, *84*, 64−76.
(23) Benchimol, S.; Fuks, A.; Jothy, S.; Beauchemin, N.; Shirota, K.; Stanners, C. P. Carcinoembryonic antigen, a human tumor marker, functions as an intercellular adhesion molecule. *Cell* **1989**, *57*, 327−334.
(24) Chen, H.; Jiang, C.; Yu, C.; Zhang, S.; Liu, B.; Kong, J. Protein chips and nanomaterials for application in tumor marker immunoassays. *Biosens. Bioelectron.* **2009**, *24*, 3399−3411.
(25) Wang, X.-W.; Xie, H. Alpha-fetoprotein enhances the proliferation of human hepatoma cells in vitro. *Life Sci.* **1998**, *64*, 17−23.
(26) Wright, L. M.; Kreikemeier, J. T.; Fimmel, C. J. A concise review of serum markers for hepatocellular cancer. *Cancer Detect. Prev.* **2007**, *31*, 35−44.
(27) Tamayo de Miguel, F. J.; Mertens, J.; Calleja Gómez, M. System and method for surface inspection of micro and nanomechanical structures. EU Patent EP053801572007.
(28) Mertens, J.; Álvarez, M.; Tamayo, J. Real-time profile of microcantilevers for sensing applications. *Appl. Phys. Lett.* **2005**, *87*, 234102−234104.
(29) Putman, C. A. J.; Grooth, B. G. D.; Hulst, N. F. V.; Greve, J. A detailed analysis of the optical beam deflection technique for use in atomic force microscopy. *J. Appl. Phys.* **1992**, *72*, 6−12.
(30) Li, C.; Zhang, M.; Zhang, Z.; Tang, J.; Zhang, B. Microcantilever aptasensor for detecting epithelial tumor marker Mucin 1 and diagnosing human breast carcinoma MCF-7 cells. *Sens. Actuators, B* **2019**, *297*, No. 126759.
(31) Holzer, B.; Manoli, K.; Ditaranto, N.; Macchia, E.; Tiwari, A.; Di Franco, C.; Scamarcio, G.; Palazzo, G.; Torsi, L. Characterization of covalently bound anti-human immunoglobulins on self-assembled monolayer modified gold electrodes. *Adv. Biosyst.* **2017**, *1*, No. 1700055.
(32) McNeillie, A.; Brown, D. H.; Smith, W. E.; Gibson, M.; Watson, L. X-ray photoelectron spectra of some gold compounds. *J. Chem. Soc., Dalton Trans.* **1980**, 767−770.
(33) Bourg, M.-C.; Badia, A.; Lennox, R. B. Gold− sulfur bonding in 2D and 3D self-assembled monolayers: XPS characterization. *J. Phys. Chem. B* **2000**, *104*, 6562−6567.
(34) Sheng, Z.-H.; Shao, L.; Chen, J.-J.; Bao, W.-J.; Wang, F.-B.; Xia, X.-H. Catalyst-free synthesis of nitrogen-doped graphene via thermal annealing graphite oxide with melamine and its excellent electrocatalysis. *ACS Nano* **2011**, *5*, 4350−4358.
(35) Vilar, M. R.; Botelho do Rego, A. M.; Ferraria, A. M.; Jugnet, Y.; Nogues, C.; Peled, D.; Naaman, R. Interaction of self-assembled monolayers of DNA with electrons: HREELS and XPS studies. *J. Phys. Chem. B* **2008**, *112*, 6957−6964.
(36) Zwahlen, M.; Brovelli, D.; Caseri, W.; Hähner, G. Orientation and electronic structure of ion-exchanged pyridinium compounds on mica. *J. Colloid Interface Sci.* **2002**, *256*, 262−267.
(37) Shard, A. G.; Whittle, J. D.; Beck, A. J.; Brookes, P. N.; Bullett, N. A.; Talib, R. A.; Mistry, A.; Barton, D.; McArthur, S. L. A NEXAFS examination of unsaturation in plasma polymers of allylamine and propylamine. *J. Phys. Chem. B* **2004**, *108*, 12472−12480.

DOI: 10.1021/acssensors.9b01604
ACS Sens. 2019, 4, 3034−3041